

Non-Statistically Populated Autoionizing Levels of Li-like Carbon: Hidden-Crossings

E. F. Deveney*, H.F. Krause, N.L. Jones, J.M. Sanders**, C.R. Vane,
W.Wu and S. Datz.

Physics Division, Oak Ridge National Laboratory, Oak Ridge, TN 37831-6377 USA

M. Breinig, D. Desai and S.Y. Ovchinnikov

*Department of Physics, The University of Tennessee, Knoxville, TN 37996-1200 USA
and Oak Ridge National Laboratory, Oak Ridge, TN 37831-6377 USA*

Q.C. Kessel

Department of Physics, The University of Connecticut, Storrs, CT 06269-3046 USA

S.M. Shafroth

*Department of Physics and Astronomy, The University of North Carolina, Chapel Hill NC
27599-3255 USA*

RECEIVED
FEB 05 1996
OSTI

Abstract. The intensities of the Auger-electron lines from autoionizing (AI) states of Li-like ($1s2s2l$) configurations excited in ion-atom collisions vary as functions of the collision parameters such as, for example, the collision velocity. A statistical population of the three-electron levels is at best incomplete and underscores the intricate dynamical development of the electronic states. We compare several experimental studies to calculations using 'hidden-crossing' techniques to explore some of the details of these Auger-electron intensity variation phenomena. Our investigations show promising results suggesting that Auger-electron intensity variations can be used to probe collision dynamics.

INTRODUCTION

It is instructive to first discuss the autoionizing levels of the Li-like configurations which will be the subjects of investigation. There are four distinct levels of ($1s2s2l$) configurations which autoionize: $(1s2s^2)^2S$, 2P and 2P both from ($1s2s2p$) [1,2], and 4P from ($1s2s2p$) with all spins aligned. The three doublets decay to the $(\{1s^2\}^1S + e_c l_c)^2L$ ground state configuration where e_c represents the energy of a continuum electron with angular momentum l_c ($l_c = L$). The quartet will also decay via an Auger-electron transition, however the decay is spin forbidden and the state is therefore metastable. Our investigations involve the measurements of Auger-electrons from these levels that were excited from $(1s^2 2s)^2S$ during ion-atom collisions and how and why the intensities vary as functions of different collision parameters.

The submitted manuscript has been authored by a contractor of the U.S. Government under contract No. DE-AC05-84OR21400. Accordingly, the U.S. Government retains a nonexclusive, royalty-free license to publish or reproduce the published form of this contribution, or allow others to do so, for U.S. Government purposes.

Ziem *et al.* [3] measured the intensities of Auger-electrons from $Li^{**} (1s2s2l)$ targets excited by protons with impact energies from 22.5 to 500 KeV using the crossed beam method. The Auger-electrons from 2S , $^2P_-$ and $^2P_+$ states formed from a single K-shell electron excitation all exhibited intensity variations as a function of the proton energy. In particular, at 22.5 KeV, the $^2P_- / ^2P_+$ intensity ratio was 1:1 while at 400 KeV the ratio had changed to 20:1. This they note is in sharp contrast to the idea of a simple statistical excitation of levels independent of the collision energy. Deveney *et al.* [2] measured and identified Auger-electrons from the series of $(1s2snl)^2L$ AI states with $n = 2, 3, \dots, \infty$ from Li-like carbon projectiles excited by He targets in 1 MeV/amu collisions and note that a simple statistical excitation of the levels is insufficient to explain the relative intensities of the Auger-electron peaks. D.H. Lee [4] observed strong energy dependent variations of the same Auger-electron lines emitted from O^{5+} and F^{6+} projectiles excited by He and H_2 targets for total collision energies between 4 and 33 MeV. The same variations are evident in Stolterfoht's work [5,6].

There has not been, to the best of our knowledge, an unambiguous explanation of all of the before mentioned Auger-electron intensity variation phenomena. In one of our present studies the 2S , $^2P_-$ and $^2P_+$ Auger-electron peak intensities from C^{3+} projectiles excited from He, Ne, Ar, Kr and Xe targets were measured. Rich intensity variations of the Auger-electron peaks were observed as a function of increasing Z. To determine what effect the target recoil charge state has on the Auger-electron intensity distribution, a coincidence experiment was done using the He system where the Auger-electrons were measured with the specific recoil charge state produced in the collision event. Again strong intensity variations were observed. A 'quasi' one-electron model was considered in which the transition probabilities for a single C^{3+} K-shell electron dynamically developing in two distinct 'outward' collision fields (corresponding to the different potential fields from C^{3+} with either the He^{1+} or He^{2+}) gives good agreement with the experimental observations. The transition probabilities are calculated using 'hidden-crossings' [7-11]. If this picture is correct, the Auger-electron intensities and variations provide a window into the collision dynamics. In a final study to further explore this picture, we compare calculations to experimental results for the intensity variation of the 2S Auger-electron as function of collision energy.

Auger-electron Intensities as a Function Noble Gas Targets

There are five spectra in figure 1 showing electrons measured from the collision systems 4.8 MeV (4 a.u. velocity) $C^{3+} + He, Ne, Ar, Kr$ and Xe [12]. This experiment was performed at the ORNL EN Tandem accelerator facility under the same conditions described in [2]. Briefly, electrons were collected from a differentially pumped gas-cell region at 10° in the laboratory frame into a double-pass parallel-plate spectrometer [13] without any deceleration. Table 1 is given along side of figure 1 to identify the states and energies (in the frame of a C^{3+} emitter) of the Auger-electrons observed [2]. In

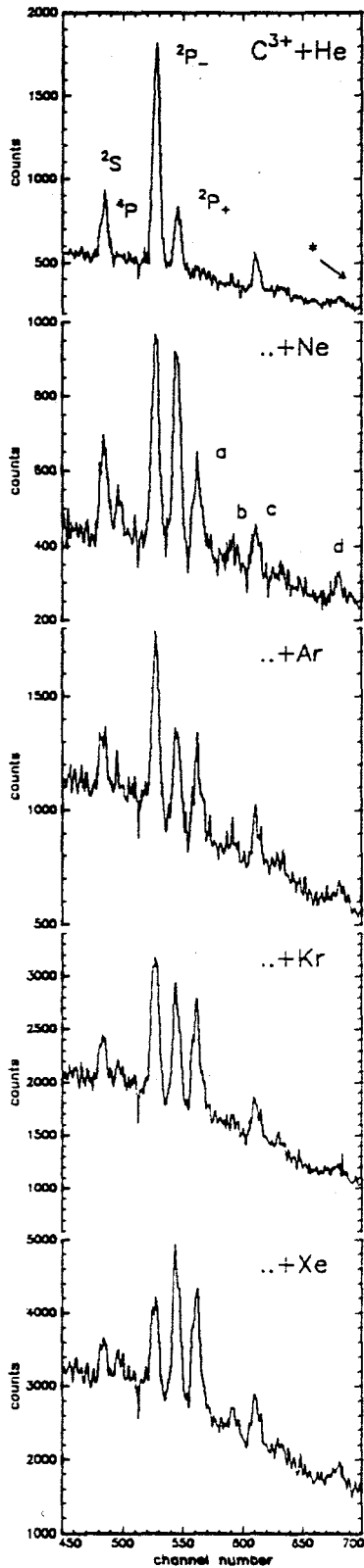


Table 1. The Auger-electron energies from doubly excited $C^{3+} (1s2snl)$ autoionizing levels, $|d\rangle$, with respect to the $(C^{4+} \{1s^2\}^1S + e_c l_c)^2L$ ground state ($l = l_c = L$) and other AI configurations (4P and a-d) observed in figure 1 [2].

line	$ d\rangle$	Auger- e^- energy (eV)
2S	$(1s\{2s^2\}^1S)^2S$	227.5
4P	$(1s2s2p)^4P$	229.9
$^2P_-$	$(1s2s2p)^2P_-$	235.9
$^2P_-$	$(1s2s2p)^2P_-$	239.3
*	$(1s2s\{n \geq 3\}l)^2L$	≥ 271

a	$(1s\{2p^2\}^1D)^2D$	242.0
b	$(1s\{2p^2\}^1S)^2S$	248.0
c	$(1s2s2p^2)^3D$ (transfer and excitation)	252.6
d	$(2s\{2s \text{ or } 2p\})$	265

Figure 1. Electrons measured at 10° in the laboratory frame from 4.8 MeV $C^{3+} + He, Ne, Ar, Kr$ and Xe collisions.

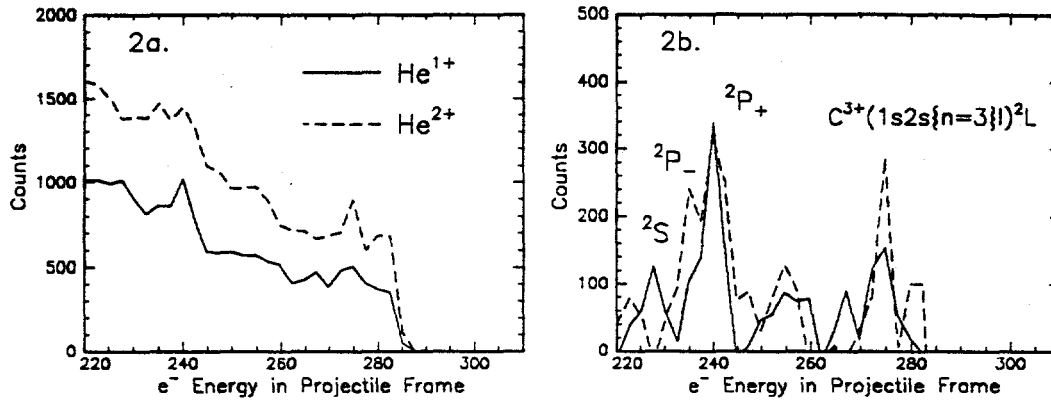
comparing the spectra it should be noted that the only parameter changed from run-to-run was the target gas.

There are intensity variations for almost all of the Auger features. The $^2P_- / ^2P_+$ intensity ratio changes from 4:1 in *He*, to 1:1 in *Ne*, to 2:1 in *Ar*, to 1:1 in *Kr* and finally to 2:3 in *Xe*. We note the absence of the 4P Auger-peak. This is attributed to its long life time, $10^{-9} - 10^{-8}$ seconds [14], which means it decays outside of the effective target length seen by the electron spectrometer [2]. In measurements of zero degree electrons from a very long effective target length (~ 20 cm) by Lee [4] the 4P is one of the dominant Auger-electron features. An important conclusion that we draw from one of Lee's studies using retarding fields to separate in energy electrons born in different parts of the target length is that the 2S , $^2P_-$ and $^2P_+$ Auger-electron intensity variations are not target length dependent.

Auger-electron and Recoil Charge State Coincidences

To investigate whether or not the particular charge state of the recoil had any effect on the Auger-electron intensity distributions we measured the 2S , $^2P_-$ and $^2P_+$ Auger-electron peaks in coincidence with either the He^{1+} or the He^{2+} recoil charge state in $C^{3+} + He$ (4 a.u. velocity) collisions. A Univ. of TN spectrometer at ORNL was used for this measurement [15]. Here, ~ 4 pA C^{3+} beam was steered through a 1 cm target gas cell maintained at 4 mTorr. Recoils were extracted at 90° and down stream at $0 \pm 10^\circ$ electrons were directed into a single pass parallel plate spectrometer and onto a two-dimensional position-sensitive-detector. A PC collected the position and coincidence information which was partitioned into three separate 64 by 64 arrays; two corresponding to those electrons in coincidence with either the He^{1+} or He^{2+} and a third for all other non- and random-coincidences. The collection time for this data set was 84 hours. The total number of electrons in coincidence with He^{1+} was approximately equal to the number in coincidence with He^{2+} . An amount due to randoms was estimated and subtracted from each of the coincidence arrays and the data was binned at the cost of a slight loss in energy resolution. At this stage, it must be noted, the data analysis is preliminary and error analysis has not been completed.

Figures 2a and 2b are the preliminary results of the coincidence measurements. The solid line represents electrons measured in coincidence with He^{1+} and the dashed line represents electrons measure in coincidence with He^{2+} in figures 2a and 2b. Fig. 2a shows the data before a binary-encounter electron (BEE) background subtraction. Fig. 2b is the data following a BEE background subtraction. The line-shape of the BEE distribution was approximated from our calculations using a CDW-EIS (continuum distorted wave - eikonal initial state) code by Reinhold [16]. The x-axis is energy in the emitter, or projectile, frame. There is good overall agreement with the energies of the Auger-electrons from table 1.



Figures 2a and 2b. Emitted-electron distributions measured in coincidence with He^{1+} and He^{2+} . In fig. 2b, a binary-encounter background has been subtracted.

There appears to be significant Auger-electron intensity variation for the 2S , $^2P_-$ and $^2P_+$ Auger-electron peaks when measured in coincidence with either He^{1+} or He^{2+} . The $^2P_-$ / $^2P_+$ intensity ratio changes drastically and the $(1s2s^2)^2S$ Auger-electron disappears in the He^{2+} spectrum in conjunction with the increase in the number of Auger-electrons from the $(1s2s3l)^{**}$ state (the peak at 273 eV). It is this later aspect of the intensity variations that we will consider more deeply.

Model and Calculations for the Intensity Variations

The coincidence measurements suggests that there is an interaction characterized by the distinct post-collision fields produced by either the He^{1+} or the He^{2+} acting on the outward C^{3+**} that plays a role in determining the final Auger-electron intensity distribution. Having selected small impact parameters (the final AI configurations, $1s2snl$, can be associated with $1s \rightarrow nl$ excitations at small impact parameters of $\sim 1/6$ a.u. for carbon) on the inward part of the collision a carbon K-shell electron will develop in the combined field of it's own nucleus and an unscreened He . If the He target is ionized quickly on the inward part of the collision by impulsive Coulomb interaction with the projectile (binary encounters), the K-shell electron will develop on the outward part of the collision in a post-collision field that depends on the ionization state of the He . The outward potential curves for C^{3+**} with either the He^{1+} or the He^{2+} are very different as are the inelastic excitations and population probabilities amongst the quasi-molecular states calculated using hidden-crossings. In the limits of the far separated atoms (ions), it is the expansion of the differently populated outward quasi-molecular levels for either the C^{3+} and He^{1+} or C^{3+} and He^{2+} systems onto the final AI atomic basis states that can lead to some of the Auger-electron intensity variations.

Hidden-crossing theory and techniques offer a means to calculate nonadiabatic or inelastic radially-coupled transitions [7-11]. In this theory, transition probabilities rely only on the evaluation of the Massey-parameter around branch points connecting different potential surfaces that are constructed from time independent eigen-value solutions to the Schrodinger equation for complex internuclear distance. The probability for a transition from an initial state, i , to a final state, j , is given by;

$$P_{i-j} = \exp \left\{ -2 \left| \frac{\Delta_{i-j}}{v_0} \right| \right\} \quad (1)$$

where Δ_{i-j} is the Massey parameter and v_0 is the collision velocity. Equation (1) is expected to give good results for $\Delta_{i-j} > v_0$. Krstic and Janev [10] used hidden-crossings to calculate $1s \rightarrow 2s$ excitations in $He^{2+} + H(1s)$ collisions up to 1.7 a.u. of internuclear velocity, which is larger than the $H(1s)$ electron velocity, with good results. It should be noted that hidden-crossing techniques have thus far only been developed for and used in one-electron systems and ours is the first extension of such techniques to a complex 'quasi' one-electron system. The potential curves for complex internuclear distances needed to evaluate the Massey parameter are numerical solutions to the three-body (two-center) instantaneous eigen-value problem. A cut of the potential surfaces with zero component of complex internuclear distance is shown in figure 3.

The first potential curve in fig. 3 takes the ion-atom collision event from an internuclear distance of minus infinity (shown starting at -5) to 0 a.u. for the inward part of the collision. The effective nuclear charges experienced by the carbon K-shell electron developing from $-\infty$ to the united atom limit are $Z^* = 5.7$ and $Z^* = 5.7 + 2$ respectively (using Slater's screening rules [17]). There is a strong radial coupling of the $1s\sigma$ to the $2p\sigma$ molecular orbital which shows up as a branch point at $0.4 + i0.3$ a.u. in the complex plane. For this coupling, the Massey parameter is 5.2 which is greater than v_0 (4.0 a.u.). This T-series coupling is characteristic of saddle-point excitation in which the electronic probability amplitudes build up on the unstable equilibrium point or saddle of the two nuclear coulomb centers. Electrons promoted to the $2p\sigma$ may also experience a rotational coupling to the $2p\pi$ that can be estimated from a model by Demkov [18]. At plus infinity, a $2p\sigma$ molecular orbital collapses into an atomic orbital resulting in a $C^{3+**}(1s2s^2)^2S$ three-electron level. Similarly, the $2p\pi$ and $2s\sigma$ electrons yield the $C^{3+**}(1s2s2p)^2P_-$ and $C^{3+**}(1s2s2p)^2P_+$ levels respectively. K-shell electrons promoted into principle quantum states, $n > 2$, develop into $C^{3+**}(1s2s\{n \geq 3\})^2L$ levels in the separated ion limit.

Also shown in fig. 3 are the outward potential curves calculated for the cases $C^{3+} + He^{1+}$ (top) and $C^{3+} + He^{2+}$ (bottom). At an internuclear distance of zero $Z^* = 4.8 + 1$ and $Z^* = 4.8 + 2$ are used as the united atom effective nuclear charges for the He^{1+} and He^{2+} cases respectively. The 4.8 is the effective charge for the $2l$

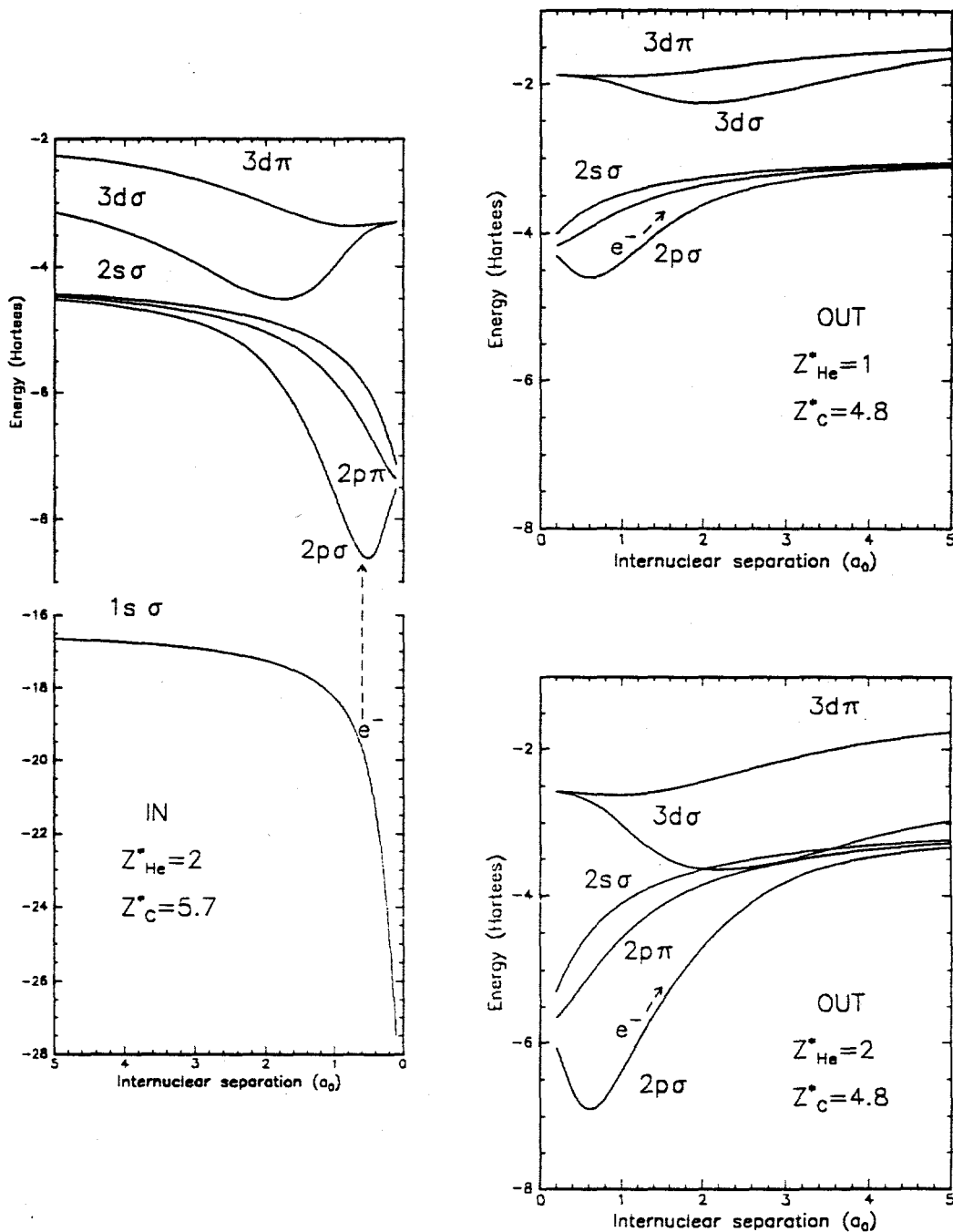


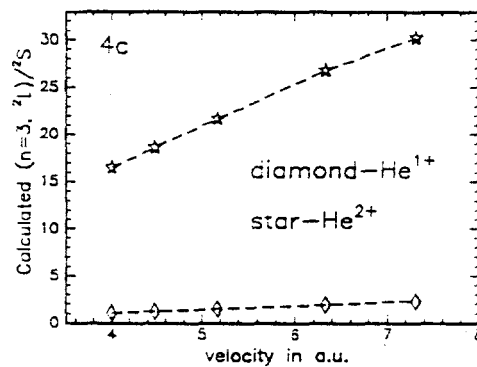
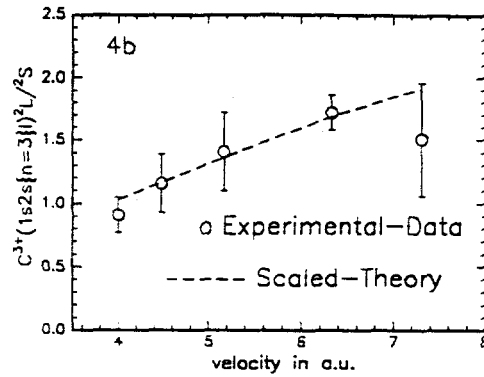
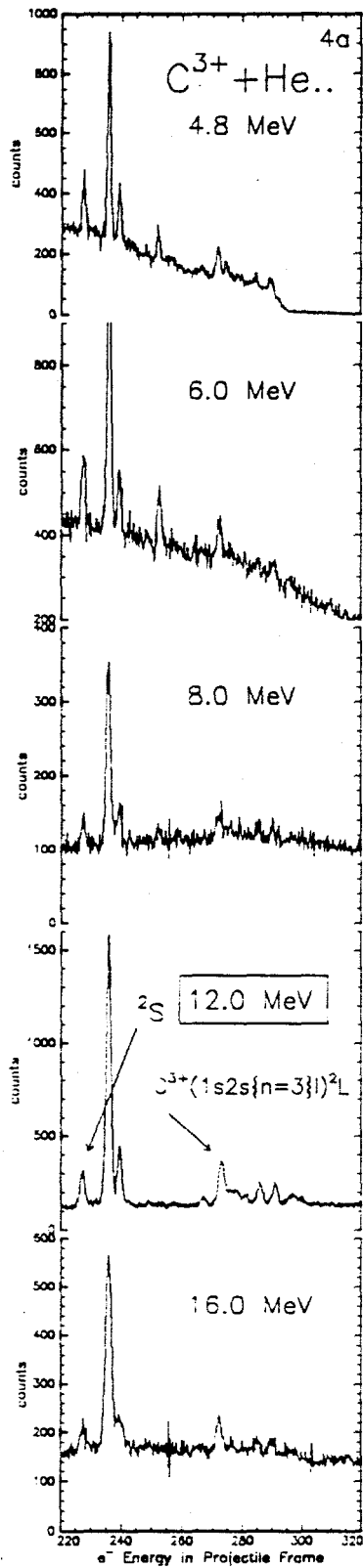
Figure 3. A single K-shell electron on an 'inward' and two distinct, corresponding to He^{1+} or He^{2+} , 'outward' potential curves.

$C^{3+}(1s2s2l)$ electron screened by a $1s$ and $2s$ electron. In both of the outward potential curves there is a branch point connecting the $2p\sigma$ level to the $3d\sigma$ level by a T-series transition at 2-4 a.u. of internuclear distance. The Massey-parameters evaluated for the $2p\sigma$ to $3d\sigma$ transitions in the He^{1+} system is 1.4 while in the He^{2+} system it is 0.12. Under these conditions the absolute probabilities might not be expected to be exact but the relative ratio of probabilities for the two cases should be good. Using equ. 1, the $2p\sigma \rightarrow 3d\sigma$ transition probability in the $C^{3+} + He^{2+}$ system is found to be 10 times larger than it is in the $C^{3+} + He^{1+}$ system. In other words, the $2p\sigma$ population (connected to the $C^{3+**}(1s2s^2)^2S$ in the separated atomic basis) is essentially dumped into the $3d\sigma$ (connected to the $C^{3+**}(1s2s\{n=3\})^2L$ population by a factor of 10 more often in He^{2+} than it is for He^{1+} . This is evident in fig. 2b; the Auger-electron intensity from $C^{3+**}(1s2s^2)^2S$ in He^{2+} has nearly vanished while the intensity of Auger-electrons from $C^{3+**}(1s2s\{n=3\})^2L$ at roughly 273 eV has increased.

Energy Variation of the 2S Auger-electron Intensity

To investigate the promotion of the $2p\sigma$ into the $n=3$ level more closely, previous singles data from the $C^{3+} + He$ system at 4.8, 6.0, 8.0, 12.0 and 16 MeV total collision energies was analyzed for energy dependence of the 2S and the $C^{3+**}(1s2s\{n=3\})^2L$ Auger-electron intensities with 227.5 and 273 eV Auger-electron energies respectively. The autoionizing level $C^{3+**}(1s2s\{n=3\})^2L$ is associated with a K-shell electron promotion into the lowest lying $n=3$ level, the $3d\sigma$, without further excitation. Figure 4a is the energy dependent Auger-electron spectra taken under the same experimental conditions as in [2]. As a function of the collision internuclear velocity, the ratios of the number of $n=3$ Auger-electrons at 273 eV divided by the number of 2S Auger-electrons are plotted (open circles) in fig. 4b.

Using equ. (1) the probabilities P_{i-f} , for $2p\sigma - 3d\sigma$ promotion and the number of $n=3$ electrons, and $1 - P_{i-f}$, electrons that stay in the $2p\sigma$ and the number of 2S electrons, are computed as a function of the internuclear velocity and for each of the two distinct outward potential fields. The ratio $P_{i-f} / (1 - P_{i-f})$, is given for each case: C^{3+} with He^{1+} and with He^{2+} (diamond and star symbols) respectively in fig. 4c. To compare with the experimental data, the calculated ratios were averaged (the singles data does not differentiate the charge state of the recoil and we have determined that the number of He^{1+} is roughly equivalent to the number of He^{2+}) and scaled down by a factor of 8.5. In fig. 4b, the comparison is made between theory, dashed curve, and experiment, open circles. There is good overall agreement between theory and experiment. Scaling the computed values down is reasonable because additional transitions out of the $3d\sigma$ and into the $n \geq 4$ levels are not taken into account.



Figures 4a, b and c. Energy dependent study of the $C^{3+}(1s2s\{n=3\})^2L$ and $C^{3+}(1s2s)^2S$ Auger-electron peaks.

Fig. 4a. Electrons at 10° measured from the $C^{3+} + He$ system at 4.8, 6.0, 8.0, 12.0 and 16.0 MeV total collision energies. In the 12 MeV data, the $(n=3,^2L)$ and the 2S are pointed out.

Fig. 4b. Comparison of the experimental ratios of the measured intensities for $(n=3,^2L)/^2S$ with our theoretical results, from fig. 4c, after averaging and scaling by $1/8.5$.

Fig. 4c. The calculated ratios of $(n=3,^2L)/^2S$ for He^{1+} recoils (diamonds) and for He^{2+} recoils (stars).

Conclusions

Having measured the Auger-electron intensity variations from $C^{3+}(1s2snl)$ levels excited in various $C^{3+}(1s^2 2s)S + atom$ collisions, we also explored the possibility that the variations can be used as a window into the detail of some of the intricate dynamical developments of electrons during collision events. A 'quasi' one-electron approximation in which a single active K-shell electron develops in different outward potential fields and whose transitions can be calculated using 'hidden-crossings' techniques shows promise for the 2S Auger-electron variation in the *He* coincidence data and for the data with *He* as a function of the internuclear velocity. One of the strongest intensity variation features observed remains unexplained: the $^2P_{1/2}/^2P_{3/2}$ intensity ratio. One possible explanation is the mixing of quasi-molecular levels on the outward part of the collision from Stark and Zeeman interactions connecting $\Delta l = 1$ and $\sigma \rightarrow \pi$ levels together respectively. In this picture, the 2S , $^2P_{1/2}$ and $^2P_{3/2}$ share the population of electrons from $n = 2$ (the $2p\sigma$, $2p\pi$ and $2s\sigma$ levels) in a complicated manner depending on the internuclear velocity, the charge state of the recoiled target and the Auger-electron launch angle. Exciting experimental and theoretical work remain for these questions.

Acknowledgments

We thank P.S. Krstic for many helpful suggestions and discussions. We also thank D.H. Lee for his help and a copy of his Ph.D. thesis. Research for the ORNL participants was sponsored by the U.S. Department of Energy, Office of Basic Energy Sciences, Division of Chemical Sciences, under contract No. DE-AC05-84OR21400 with Lockheed Martin Energy Systems, Inc. Research for E.F.D., J.M.S., and W.W. was supported in part by an appointment to the ORNL Postdoctoral Research Associates Program administered by Oak Ridge Institute for Science and Education and ORNL.

* Present address: Dept. of Physics, The University of Connecticut, Storrs, CT 06269 USA.

** Present address: Dept. of Physics, The University of South Alabama, Mobile, AL 36688 USA.

References

- [1] Cowan, R.D., *The Theory of Atomic Structure and Spectra*, Cal., Univ. of Cal. Press, 1981.
- [2] Deveney, E.F. *et al.*, Phys. Rev. A, **48**, 2926-2933, 1993.
- [3] Ziem, P., *et al.* J. Phys. B: Atom. Molec. Phys. **13**, 2071-2081, 1980.
- [4] Lee, D.H., Ph.D thesis, Kansas State University, 1990.
- [5] Stolterfoht, N., Physics Reports, **146**(6), 315-424, 1987.
- [6] Stolterfoht, N., *et al.*, Phys. Rev. A, **48**, 2986-2994, 1993.
- [7] Solov'ev, E.A., Sov. Phys. Usp. **32** (3), 228-250, 1989.
- [8] Grozdanov, T.P. and Solov'ev, E.A., Phys. Rev. A, **42**, 2703-2718, 1990.
- [9] Ovchinnikov, S.Y., Phys. Rev. A, **42**, 3865-3877, 1990.
- [10] Krstic, P.S. and Janev, R.K., Phys. Rev. A, **47**, 3894-3912, 1993.
- [11] Pieksma, M., Ph.D. thesis, Utrecht University, 1993.
- [12] Deveney, E.F. *et al.*, Abstracts papers of the 18th ICPEAC Vol. 2, 499, 1993.
- [13] Bechthold, U., Masters thesis, The University of Frankfurt, 1991.
- [14] Davis, B.F. and Chung, K.T., Phys. Rev. A, **39**, 3942-3955, 1989.
- [15] Desai, D., Ph.D. thesis, The University of Tennessee, 1996.
- [16] Reinhold, C., CDW-EIS program, private communication
- [17] Slater, J.C., Phys. Rev., **36**, 57, 1930.
- [18] Demkov, Y.N., Kunasz, C.V. and Ostrovskii, V.N., Phys. Rev. A, **18**, 2097-2105, 1978.

DISCLAIMER

This report was prepared as an account of work sponsored by an agency of the United States Government. Neither the United States Government nor any agency thereof, nor any of their employees, makes any warranty, express or implied, or assumes any legal liability or responsibility for the accuracy, completeness, or usefulness of any information, apparatus, product, or process disclosed, or represents that its use would not infringe privately owned rights. Reference herein to any specific commercial product, process, or service by trade name, trademark, manufacturer, or otherwise does not necessarily constitute or imply its endorsement, recommendation, or favoring by the United States Government or any agency thereof. The views and opinions of authors expressed herein do not necessarily state or reflect those of the United States Government or any agency thereof.